CHIN. PHYS. LETT. Vol. 34, No. 3 (2017) 035201

Ramp-Wave Compression Experiment with Direct Laser Illumination on ShenGuang-Ⅲ Prototype Laser Facility *

Feng Wang(王峰)[1,2], Quan-Xi Xue(薛全喜)[1,3], Teng Ji(纪腾)[1], Yu-Long Li(理玉龙)[1,2]**, Tao Xu(徐涛)[1,2], Xiao-Shi Peng(彭晓世)[1,2]

[1]*Research Center of Laser Fusion, China Academic of Engineering and Physics, Mianyang 621900*
[2]*Collaborative Innovation Center of IFSA, Shanghai Jiao Tong University, Shanghai 200240*
[3]*State Key Laboratory of Laser Interaction with Matter, and Northwest Institute of Nuclear Technology, Xi'an 710024*

(Received 6 June 2016)

Ramp-wave compression experiment to balance the high compression pressure generation in aluminum and x-ray blanking effect in transparent window is demonstrated with an imaging velocity interferometer system for any reflector (VISAR) on ShenGuang-Ⅲ prototype laser facility. The highest pressure is about 500 GPa after using the multilayer target design Al/Au/Al/LiF and ∼10^{13} W/cm^2 laser pulse illuminated on the planar Al target, which generates the spatial uniformity to <1% over 500 μm on the ablation layer. A 2-μm-thick Au layer is used to prevent the x-ray from preheating the planar ablation Al layer and window material LiF. The imaging VISAR system can be used to record the abrupt loss of the probe beam (λ = 532 nm) caused by absorption and reflection of 20-μm, 30-μm and 40-μm-thick Al, i.e., the blanking effect. Although there are slight shocks in the target, the peak pressure 500 GPa, which is the highest data up to now, is obtained with ramp-wave compression.

PACS: 52.35.Tc, 52.50.Lp, 62.50.−p DOI: 10.1088/0256-307X/34/3/035201

The properties of materials under high pressure and high strain rate, such as those in the planet core, are important for geosciences and material science. However, it is very difficult for them to be studied in laboratories.[1−6] The ramp-wave compression (RWC) technique is a valuable approach to generate a material under high pressure, to determine its properties such as the equation of state (EOS) and dynamic plasticity, and to test the corresponding theoretical models as well. Recently, RWC has been demonstrated to be a technique for applications in such as magnetic-pulse loading,[7,8] graded density impactors on gas gun facilities,[9] chemical energy of high explosives,[10] and pulse-shaped laser drives.[11,12] The characteristic loading time is ∼100 ns for magnetic ramp loading, ∼1 μs for graded-density impactor loading, and ∼10 ns for laser ramp loading.

The traditional RWC[1−12] requires that the compression should be gentle, and great efforts have been made to eliminate the slight shocks. However, in the laser drive RWC experiment, the conflict between eliminating the preheat effect, obtaining the high pressure and enhancing the efficiency of laser-pressure, leads to a new target concept to allow some slight shocks in RWC, other than to remove them. Since the discrepancy between the ideal and true compression waves cannot be avoided, a target Al/Au/Au/LiF has been presented to balance the high compression pressure generation in aluminum and x-ray blanking effect in transparent window. To achieve higher ablation efficiency and lower blanking effect, the ablation layer Al was attached to the high Z Au layer. Although there will be some slight shocks in Al/Au due to the impedance mismatch, these shocks are expected to be small enough to be accepted. For the laser drive RWC experiment, the direct laser illumination is one of the most efficient techniques since the laser energy can be transferred to the target without additional loss. With the techniques presented above, a direct laser-drive shock-RWC was demonstrated in the ShenGuang-Ⅲ prototype laser facility.

In the previous laser-driven RWC experiments,[2] the unplanar pressure loading and x-ray preheating-caused blanking effect in the transparent window (LiF or quartz) had limited their applications in EOS measurements. To generate high pressure in aluminum, and at the same time to eliminate the x-ray blanking effect in the transparent window, we design 20 μm/30 μm/40μm-thick Al targets to find out the proper thickness. The laser-produced x-ray-drive ramp-wave compression is of spatial uniformity to <1% over 500 μm. This uniform loading ensures that different thicknesses of the multi-thickness targets has the same loading history.

Figure 1 shows the schematic diagram of our experiment. The four laser beams (energy 1300 J, wavelength 351 nm) to form a ϕ2 mm focus shape from an x-ray pinhole camera (XPHC) illuminated on the Al layer of the target, and the line-imaging velocity interferometer (VISAR)[13,14] with a probe laser (λ = 532 nm) received the reflected signal from the 500-μm-thick LiF window. Three targets of Al/LiF with the 20 μm/30 μm/40 μm-thick Al are the main targets. The high-Z material Au was used to prevent the transparent window from the blanking effect.

In the RWC experiment, the sample thickness should be designed carefully. The compression wave will become the shock wave in a certain position.

*Supported by the National Natural Science Foundation of China under Grant No 11305160.
**Corresponding author. Email: 2013may6th@sina.com
© 2017 Chinese Physical Society and IOP Publishing Ltd

There are mainly three Al thicknesses for manufacture of the targets. The Al sample was a 20-μm, 30-μm, and 40-μm-thick stepped foil attached to the LiF window, which has been turned with 20-μm, 30-μm, and 40-μm-thick Al in advance. Au is a spurting film on the Al sample. Lastly, a 10-μm-thick Al was attached to the Au layer. Through each stage of the process, a white-light interferometry was used to ensure a surface roughness smaller than 0.2 μm, overall thickness gradients smaller than 1%, and thickness of each layer smaller than 1%.

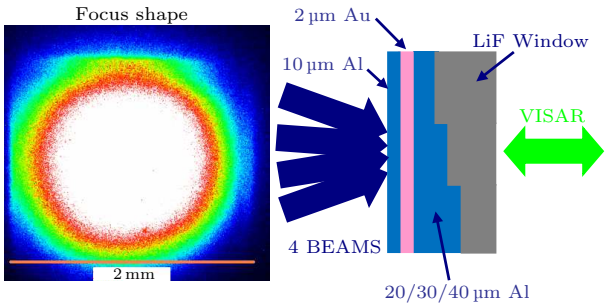

Fig. 1. (a) Laser spot shape with x-ray camera. (b) Schematic diagram of Al/Au/Al/LiF in the RWC experiment with laser direct driving.

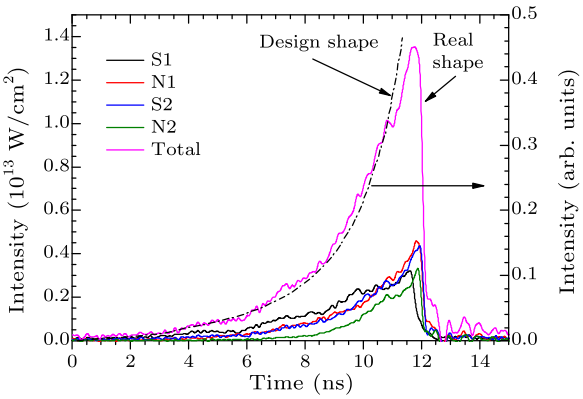

Fig. 2. Comparison of design and experimental laser shape.

A new laser shape should be designed to reach the certain state with the Al/Au/Al/LiF structure. If the real shape has some deviations from the design shape, the certain position will be less than the design data. From this basic physics process, the general RWC pressure followed[9] after the RWC laser shape has been considered,

$$p(t) = \frac{\rho_0 c_0^2}{\gamma}\left[\left(1 - \frac{t}{t_0}\right)^{\frac{-2\gamma}{\gamma+1}} - 1\right], \qquad (1)$$

where ρ_0 and c_0 are the density and sound velocity in a normal state, t is the time when the shock wave occurs, t_0 is the time of laser pulse, and $c_0 t_0$ is the theoretical thickness for the most compression position. As a laser directly driven, a scaling relation[10,11] $p(\text{Mbar}) = 0.40 I_{\text{L}}^{2/3} \lambda_{\text{L}}^{-2/3} (A/2Z)^{1/3}$ should be followed, where the unit of I_{L} is TW/cm^2, A is the quality parameter, and Z is the atomic number. Combining the two relations, the laser shape can be obtained to read

$$I_{\text{L}} = 4.16(A/2Z)^{-1/2} \lambda_{\text{L}} \rho_0^{3/2} c_0^3 \gamma^{-3/2} \times 10^{-3}[(1 - t/t_0)^{-2\gamma/(\gamma+1)} - 1]^{3/2}, \qquad (2)$$

where $t = 14$ ns, $t_0 = 12$ ns, $c_0 = 5.328$ km/s,[10] $\rho_0 = 2.70$ g/cm^3, and $\gamma = 3.505$.

Figure 2 shows the design laser shape and the real experimental shape. The design shape plotted in Fig. 2 is calculated from Eqs. (1) and (2). The real shape 'total' shows the composition of different laser beams (S1, N1, S2 and N2). As shown in Fig. 2, it is found that there are some deviations between the design shape and the real shape. Although the deviation is very small, the position where the shock wave appears will be less than the designed data.

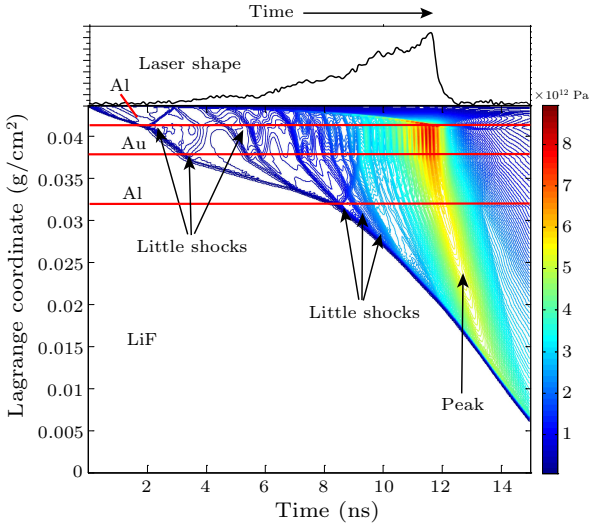

Fig. 3. Pressure distribution in the target. Upset shows the laser shape. The slight shocks are generated by the impedance unmatching of Al/Au, Au/Al and Al/LiF. The peak can be measured at about 12 ns.

The pressure in the Al/Au/Al/LiF target was simulated with the Multi-1D program, as shown in Fig. 3. The thicknesses of target layers of Al/Au/Al/LiF are 10 μm, 2 μm, 20 μm and 120 μm, respectively. The laser pulses come from the experimental measurement, which are about 12 ns in width. To avoid the preheat effect, a 2-μm-thick Au layer is used to shield the x-ray generated by the ablation layer. The highest laser intensity is $\sim 10^{13}$ W/cm^2. From Fig. 3, it is found that there are many 'slight shocks' at Al/Au, Au/Al and Al/LiF interfaces due to the unmatched impedance. There is an obvious 'peak' in 12 ns in the Al–LiF interface. For the shocks' RWC, these slight shocks would cause the temperature to increase. Since the unmatched impedance to avoid the preheat effect cannot be diminished up to now for laser direct driving, the temperature increasing produced by slight shocks should be considered as a part of the RWC compression. Then we call this kind of experimental technique the shocks' RWC.

When the slight shock and peak compression waves reach the interface of the Al/LiF (shown in Fig. 3), the interface would accelerate into the LiF window, and the interface velocity history u for each layer was recorded with a line-imaging velocity interferometer (VISAR).[13,14] A typical VISAR data recorded (Fig. 4) has a spatial resolution of ~4 μm over 500 μm at the target, a temporal resolution 0.01 ns over an 20 ns window, and a minimum velocity per fringe of 2.87 km/s with the fringe position determined to less than 2% of a fringe.

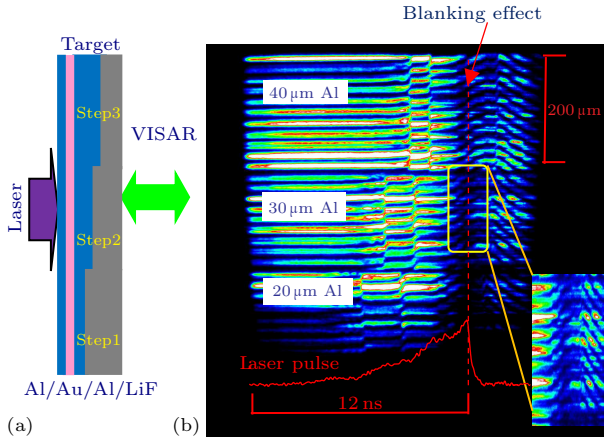

Fig. 4. (a) Schematic diagram of the Al/Au/Al/LiF target. (b) Experimental fringe of three Al thicknesses with the blanking effect. The blanking effect is obvious when the laser pulse increases to the highest intensity. The fringe is for the 30-μm-thick Al in detail.

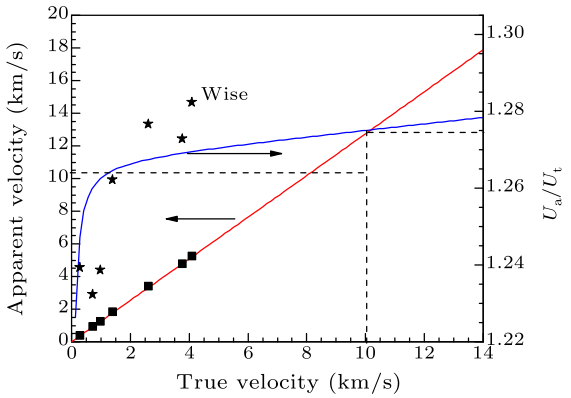

Fig. 5. The dynamic correcting curve between apparent particle velocity and real particle velocity in the LiF window. Solid rectangles and stars show the experimental data from Ref. [15]. U_a/U_t means the ratio of apparent velocity and true velocity in the LiF window.

Figure 4 shows the representative fringe histories for 20-μm, 30-μm, and 40-μm-thick Al. The preheating effect can be observed obviously. For this experiment with imaging VISAR, x-rays generated by laser ablating on the target would cause a brief period of photoionisation in the transparent material, which is called the blanking effect.[13] This blanking effect will lead to a dark area in the timescale of the optical streak camera (OSC). Moving fringe shows the acceleration and deceleration of particle velocity. For the 20-μm-thick Al, the blanking effect is too serious to obtain the interface velocity from the fringe data. For the 30-μm-thick Al, the blanking effect is better than that for the 20-μm-thick Al. Then the fringe S/N (ratio of signal and noise) of the 30-μm-thick Al may be the limitation of this kind of target design.

The correction index of the refractive is obtained from the other experiments,[15,16] as shown in Fig. 5. After comparing the apparent particle velocity and the true particle velocity in the reference, the dynamic correcting curve can be obtained to achieve the real particle velocity, which is more accurate. In our experiment, the correction index changes from 1.23 to 1.275 when we process the fringe data to obtain the 'true' interface velocity.

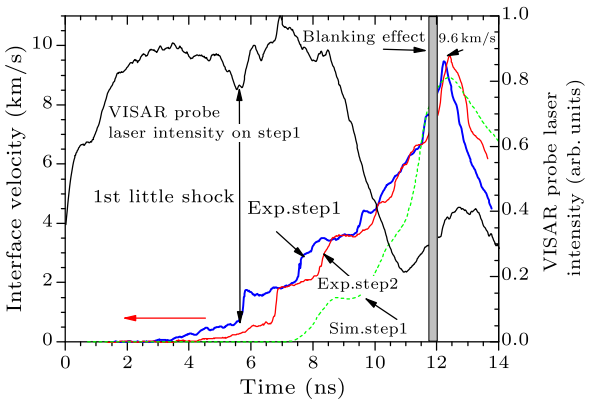

Fig. 6. The interface velocity of the three Al thicknesses. The slight shocks are caused by the impedance unmatching and laser deviation. Exp.step1 and Exp.step2 are the experimental data of 30-μm and 40-μm-thick Al, respectively. Sim.step1 is the simulation data of 30-μm-thick Al.

The Fourier transform method is the typical method to process the fringe in Fig. 4. We use the 'flood' algorithm to unwrap the phase. The interface velocities of 30-μm and 40-μm-thick Al are shown in Fig. 6. The dashed line in Fig. 6 shows the laser intensity variation along the timescale. The blanking effect causes the intensity up to 0.2, which may be the limitation for the fringe S/N. From Fig. 6, the highest particle velocity is 9.6 km/s for the 30-μm-thick Al. There are some fluctuations along the particle velocity curve which has been shown in other works.[1,2]

As reported in Ref. [17], when the shock wave velocity is higher than 18 km/s, the reflected surface to the VISAR system is the shock front, rather than the interface of Al/LiF. Thus if the apparent velocity from the peak shock is higher than 18 km/s in our experiment, the shocks' RWC has transformed to shock compression. Thus we should control the shocks' RWC experiment with the shock-less experimental regime.

The Lagrangian analysis method developed by Aidun *et al.*[18] and modified by Rothman *et al.*[19,20] is used to determine the Lagrangian sound speed $C_L(u)$. Its uncertainty is obtained from this position-time data by linear regression using errors determined

by measurement accuracies: ($u \sim 0.2$ km/s), time (∼10 ps), each layer thickness (∼1%). The compression pressure is obtained by $P_x = \rho_0 \int_0^u \langle C_{\rm L} \rangle du$.[1]

However, there are reverberation shocks in the samples due to the three Al thicknesses. In this study, we use a characteristic method called the Murnaghan-form isentropic equation[21] to improve the traditional Lagrangian method. Then the characteristic reverberation and transmission on an interface and characteristic intersection are analytically described.[22] The process data to obtain the pressure in the target is shown in Fig. 7. In Fig. 7, the experiment is calculated with the characteristic method.[22] The parameters for the materials in the Murnaghan-form are corrected with the interface velocity curves of two Al thicknesses in Fig. 4. Thus the calculated curve should be regarded as the experimental data with the error bar. Since the density is increasing with the interface velocity, the error bars of pressure and density deviations in the LiF, which are deduced by the Mie–Grüneisen equation, will be enlarged.

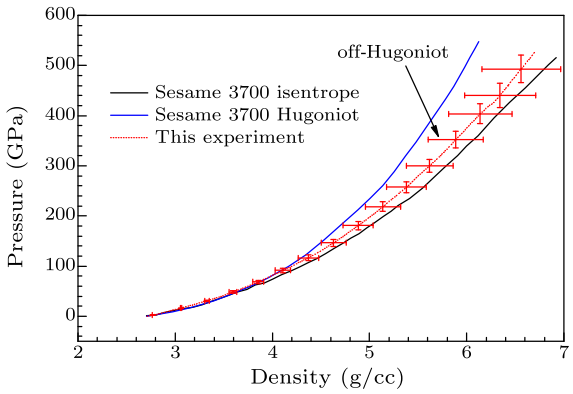

Fig. 7. Comparison of the pressure density curves of the Sesame 3700 data and the present experiment. The error bars identify the data range.

Figure 7 shows the pressure-density curve from the simulation with the Sesame 3700 database. The pressure-density curve of the present experiment is higher than the Sesame 3700 Hugoniot line and lower than the Sesame 3700 isentropic line. The pressure-density curve is the obvious reference data to confirm the RWC experiment. Along the timescale, the RWC line deflects the isentropic line as the density increases. This means that the degree of RWC of the Sesame 3700 isentropic line is not as good as that designed in our experiment.

In summary, we have proposed a new target concept to develop a laser-driven shocks' RWC technique for studying material behavior under dynamic high-pressure conditions. As the slight shocks in our experiment cannot be avoided, the effort to diminish the shock under a special level has been demonstrated with an Al/Au/Al/LiF target. Because the x-rays passed through the Al layer have been blocked by the Au layer, the blanking effect on the OSC with the target design of 30-μm-thick Al and LiF window may be greatest for this kind of RWC experiments. With the design laser shape and target structure of Al/Au/Al/LiF, 500 GPa may be the highest pressure after balancing the preheat effect and ablation efficiency for laser direct-drive experiment.

References

[1] Ao T, Knudson M D, Asay J R and Davis J P 2009 *J. Appl. Phys.* **106** 103507
[2] Lorenz K T, Edwards M J, Jankowski A F, Pollaine S M, Smith R F and Remington B A 2006 *High Energy Density Phys.* **2** 113
[3] Swift C 2008 *J. Appl. Phys.* **104** 073536
[4] Swift C and Johnson P 2005 *Phys. Rev.* E **71** 066401
[5] Park H, Remington B A, Braun D, Celliers P, Collins G W, Eggert J, Giraldez E, Le S, Lorenz T, Maddox B, Hamza A, Ho D, Hicks D, Patel P, Pollaine S, Prisbrey S, Smith R, Swift D and Wallace R 2008 *J. Phys.: Conf. Ser.* **112** 042024
[6] Smith F, Eggert Jon H, Jankowski A, Celliers P M, John M, Gupta Y M, Asay J R and Collins G W 2007 *Phys. Rev. Lett.* **98** 065701
[7] Davis J P 2006 *J. Appl. Phys.* **99** 103512
[8] Hayes D B, Hall C A, Asay J R and Knudson M D 2004 *J. Appl. Phys.* **96** 5520
[9] Asay J R 1997 *Int. J. Impact. Eng.* **20** 27
[10] Barnes J F, Blewett P J, McQueen R G, Meyer K A and Venable D1974 *J. Appl. Phys.* **45** 727
[11] Loren K T z, Edwards M J, Glendinning S G, Jankowski A F, McNaney J, Pollaine S M and Remingtin B A 2005 *Phys. Plasmas* **12** 056309
[12] Bradley D K, Eggert J H, Smith R F, Prisbrey S T, Hicks D G, Braun D G, Biener J, Hamza A V, Rudd R E and Collins G W 2009 *Phys. Rev. Lett.* **102** 075503
[13] Wang F, Peng X S, Liu S Y, Xu T, Mei L S, Jiang X H and Ding Y K 2011 *Rev. Sci. Instrum.* **82** 103108
[14] Wang F, Peng X S, Xue Q X, Xu T and Wei H Y 2015 *Acta Phys. Sin.* **64** 085202 (in Chinese)
[15] Fratanduono D E, Boehly T R, Barrios M A, Meyerhofer D D, Eggert J H, Smith R F, Hicks D G, Celliers P M, Braun D G and Collins G W 2011 *J. Appl. Phys.* **109** 123521
[16] Wise J L and Chhabildas L C 1985 *Sandia National Laboratory, Albuquerque, NM, Report SAND-85-0310C, NTIS Order No DE85015505*
[17] Hicks D G, Celliers P M, Collins G W, Eggert J H and Moon S J 2003 *Phys. Rev. Lett.* **91** 035502
[18] Aidun J B and Gupta Y M 1991 *J. Appl. Phys.* **69** 6998
[19] Rothman S D, Davis J P, Maw J, Robinson C M, Parker K and Palmer J 2005 *J. Phys.* D **38** 733
[20] Rothman S D and Maw J 2006 *J. Phys. IV France* **134** 745
[21] Li W X 2003 *One-Dimensional Nonsteady Flow and Shock Waves* (Beijing: Defense Industry Press)
[22] Xue Q X, Wang Z B, Jiang S E, Ye X S and Liu J R 2014 *AIP Adv.* **4** 057127